Chapter 9

Time–Temperature Superposition Principle and its Application to Biopolymer and Food Rheology

J. Ahmed
Food and Nutrition Program, Environment and Life Sciences Research Center, Kuwait Institute for Scientific Research, Kuwait City, Kuwait

9.1 INTRODUCTION

Properties of viscoelastic materials are influenced by both measurement temperature and time (frequency). Under a constant stress/load, the deformation or strain (compliance) shown by the material will increase over a period of time due to molecular rearrangement. Therefore, the compliance or modulus measurements carried out over a short time period could generate a data that is either overestimated or underestimated. Therefore, it is essential to obtain data over a rather wide temperature and time range to characterize such materials completely and to achieve satisfactory results about the actual processing behavior. In reality, it is really difficult to measure the material for such a long period of time and a broader range of frequencies. However, the rate of such deformation or strain measurement can be accelerated by a thermally activated process to obtain the failure of materials within a limited period. It is possible to obtain deformation or strain curves at different temperature levels which can be shifted along the time axis to generate a single curve known as a master curve, from which force-deformation or strain data can be obtained. This technique is known as time–temperature superposition (TTS).

Superposition is commonly used for materials which have no universally accepted mechanistic theory (Markovitz, 1975). Sometimes it is believed that if it were an established general law of nature, examination of the data clearly shows that this is not the case. The time–temperature superposition principle (TTSP) is referred to by different names including frequency–temperature superposition,

Advances in Food Rheology and Its Applications. http://dx.doi.org/10.1016/B978-0-08-100431-9.00009-7

time–temperature analogy, method of reduced variables, time-translation equivalence, and many more. The TTSP was first reported in the work of Aleksandrov and Lazurkin (1939); later on Leaderman (1943) drew attention to the temperature shift. According to Leaderman (1943), the time is equivalent to temperature for viscoelastic materials. The concept was originally developed for polymers, and now it has been applied to virtually every mechanical property and every kind of polymer including blend. At the beginning, the technique was employed to the relaxation modulus and creep compliance. Later on, the concept has been broadened to other measurement areas of rheology including steady flow, oscillatory rheology, nonlinear viscoelasticity properties, and tensile strength to their variation with compositional and structural parameters. At the beginning, it was believed that TTSP can only be applied to amorphous thermoplastics with linear viscoelasticity in the temperature region corresponding to the rubbery state. However, the principle has been extended to crosslinked, crystalline, and even inorganic polymers (Urzhumtsev, 1972). Attempts have been made to develop a unified method of covering a broader temperature interval, including the rubbery and glassy regions. Interestingly, efforts have been made to extend the principle to materials with nonlinear viscoelasticity also.

In creep analysis, the shear creep compliance (J) measures the linear viscoelasticity behavior of the material as a function of time (t) (Fig. 9.1). When the compliance is plotted on a logarithmic scale, it is observed empirically that the curves obtained at different temperatures have similar shapes, and therefore, may be superposed by translating (commonly called shifting) the curve for the creep compliance at one temperature onto that at another temperature (Markovitz, 1975).

In linear viscoelasticity, it is customary to discuss superposition on the basis of relaxation spectra and especially on the hypothesis that all the

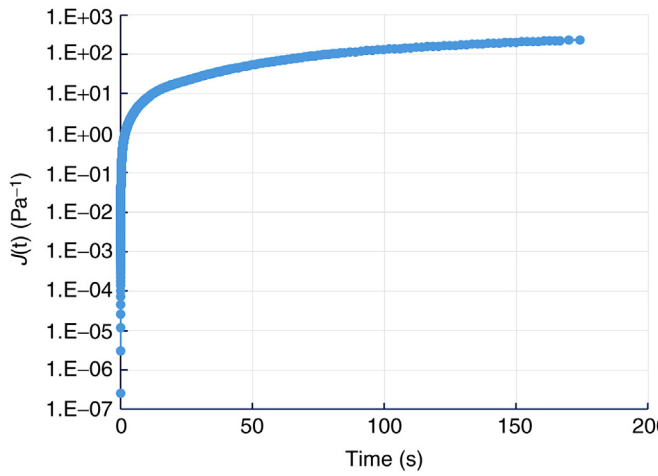

FIGURE 9.1 Typical creep behavior of a biopolymer.

relaxation times have the same temperature dependence (Markovitz, 1975). In small amplitude oscillatory shear measurement, a series of isothermal curves that correlate rheological moduli (elastic modulus, G'; viscous modulus, G''; and complex viscosity, η^*) with the range of measurement frequency (ω) can be brought together on a single master curve at a reference temperature by means of "TTS." According to the TTSP, the frequency (or response time) function of rheological modulus at a particular temperature, is very similar in shape to the same functions at adjacent temperatures. The curve of modulus against logarithmic loading frequency or logarithmic response time at one temperature can be horizontally shifted along the frequency (or the reduced time) axis, thereafter, superimposed on the curves at next temperatures. The shift along the logarithmic frequency axis is termed as the frequency–temperature shift factor a_T and the vertical temperature shift factor b_T that results from the changes in sample density with temperature ($T_0\rho_0/T\rho$); the magnitude of b_T is usually close to unity and is often neglected. Materials that require a vertical shift factor to generate a smooth master curve are classified as thermorheologically complex materials (TCMs) (Alwis and Burgoyne, 2006). The principle has found suitability among polymer and its blends, food, and biopolymers (Al-Ruqaie et al., 1997; Ptaszek and Grzesik, 2007; Mendieta-Taboada et al., 2008; Ptaszek et al., 2009; Kasapis et al., 2000; Ahmed et al., 2010; Ahmed, 2012, 2015). Sometimes, TTSP fails for various polymer/biopolymer blends because of different temperature-dependent relaxation mechanisms for each component of the blends. However, it could be achievable by increased compatibilization which generates strong phase interactions between blend components which in turn can result in single temperature dependence.

9.2 TIME–TEMPERATURE SUPERPOSITION FOR VISCOELASTIC MATERIALS

According to Rouse theory the temperature affects the relaxation modulus by changing the relaxation times (λ) by the same factor at a reference temperature of T_0 [eg, $\lambda_1(T_0)$, $\lambda_2(T_0)$, and so on], and also by changing the temperature to another value of T, where these times will be changed to $\lambda_1 a_T$, $\lambda_1 a_T$, and so on, where a_T is a function of T and is equal to unity at T_0. The shift factor, a_T depends on both T and T_0. Therefore,

$$\lambda_i(T) = a_T \lambda_i(T_0) \tag{9.1}$$

The Rouse theory furthermore directs that the magnitude of the coefficients, G_i, are also influenced by the temperature as shown next.

$$G_i(T) = G_i(T_0)\frac{T\rho}{T_0\rho_0} \tag{9.2}$$

where ρ and ρ_0 are density at a temperature T and a reference temperature T_0, respectively. Using previous equations, the relaxation modulus of a generalized Maxwell fluid can be expressed as

$$G(t;T) = \frac{T\rho}{T_0\rho_0}\sum_{i=1}^{N} G_i(T_0)\exp\left\{\frac{-t}{[\lambda_i(T_0)a_T]}\right\} \tag{9.3}$$

It can be written as

$$G_r(t) \equiv G(t;T)\frac{T_0\rho_0}{T\rho} \tag{9.4}$$

where

$$t_r = \frac{t}{a_T} \tag{9.5}$$

Furthermore, we can write

$$G_r(t_r) = \sum_{i=1}^{N} G_i(T_0)\exp\left\{\frac{-t_r}{[\lambda_i(T_0)]}\right\} \tag{9.6}$$

This equation infers that if G_r is plotted as a function of t_r, data taken at selected temperatures should fall on the same curve as those taken at the reference temperature, T_0.

According to Dealy and Wissbrun (1999) when the a_T function cannot be predicted from Rouse principle it can be determined empirically as a "shift factor." A plot of G (or log G) versus log t, a_T can be obtained from the horizontal shift necessary to bring the data for any temperature T to the same curve as data for the temperature T_0.

If Eq. 9.6 is assumed to be valid for all values of t_r, it can be used, together with the Boltzmann superposition principle, to show that all linear viscoelastic properties obey a TTSP (Edwards, 1967).

9.3 TTSP FOR MATERIALS FOLLOWING LINEAR VISCOELASTIC PROPERTIES (MARKOVITZ, 1975)

When a shear relaxation modulus curve $G(t;T_0)$ for a material at temperature T_0 is superposed on the curve $G(t;T)$ for the temperature T over a time period of t by a horizontal shift in a logarithmic plot, then the results can be expressed by the following equations.

$$G(\log t;T) = G(\log t - \log a_T;\, T_0) \tag{9.7}$$

$$G(t;T) = G\left(\frac{t}{a_T};\, T_0\right) \tag{9.8}$$

The term $G(\log t;T)$ is employed when explicit reference to the logarithmic abscissa is required. The horizontal displacement of the two curves in the logarithmic plot is $\log a_T$ which is known as the horizontal shift factor.

In some cases, it requires to transpose the curves of a logarithmic plot in a vertical direction by an insignificant amount, $\log b_T$, where b_T is termed the vertical shift factor. This is written as

$$\log G(\log t;T) + \log b_T = \log G(\log t - \log a_T; T_0) \tag{9.9}$$

$$b_T G(t;T) = G\left(\frac{t}{a_T}; T_0\right) \tag{9.10}$$

If the previous relation fits well, it can be inferred that the temperature superposition is valid for $G(t;T)$ over a selected range of t and T. If Eq. 9.10 fits well for all values of t for a material, the material is considered as a thermorheologically simple. The term thermorheologically simple refers to the key caveat that all relaxation times of the polymer must be affected by temperature in the same way. This assumption has been found true for a wide range of homopolymers.

Furthermore, Eq. 9.10 infers that if the relaxation modulus is plotted as $b_T G(t;T)$ against t/a_T, the curves at selected temperatures will overlap over a range of values of t and will correspond to $G(t;T_0)$, the relaxation modulus function at T_0. Such a plot is termed as a reduced or master curve; $b_T G(t;T)$ is called the reduced shear relaxation modulus $G_r(t;T)$, and t/a_T is called the reduced time t_r. Eq. 9.10 is thus written as

$$G_r(t;T) = b_T G(t;T) = G\left(\frac{t}{a_T}; T_0\right) = G(t_r; T_0) \tag{9.11}$$

If $G(t;T)$ is valid for a linear viscoelastic material, the other shear viscoelastic moduli [eg, $G'(\omega;T)$, $G''(\omega;T)$, $J(\omega;T)$, and $\eta^*(\omega;T)$] can be determined by similar relationships from Boltzmann's phenomenological theory of linear viscoelasticity. Then time–temperature equivalence for one of the shear viscoelasticity properties has similar implications for the others.

9.4 ELASTIC MODULUS AND RELAXATION MODULUS SUPERPOSITION

By using Boltzmann's equation, the $G'(\omega;T)$ can be expressed in terms of the shear relaxation modulus $G(t;T)$ through the sine Fourier transforms for all values of T, t, and ω:

$$G'(\omega;T) = \left[G_e(T)\right] + \omega \int_0^\infty \left\{G(t;T) - \left[G_e(T)\right]\right\} \sin \omega t \; dt \tag{9.12}$$

Here, $G_e(T)$, defined as the limiting value of $G(\infty;T)$ for the viscoelastic solid, is also seen to be the low frequency limit of $G'(\omega;T)$:

$$G_e(T) = G'(0;T) \tag{9.13}$$

If superposition is valid for all t values over a temperature range that includes T and T_0, it is then seen from Eq. 9.11 that, for the viscoelastic solid

$$G_e(T_0) = b_T G_e(T) \tag{9.14}$$

By considering the limit at infinite time, substitution of Eqs. 9.11 and 9.14 into Eq. 9.12 leads to

$$G'(\omega;T) = \left\{\left[G_e(T_0)\right] + \omega \int_0^\infty \left\{G\left(t/a_T;T_0\right) - \left[G_e(T_0)\right]\right\} \sin\omega t \; dt\right\} / b_T \tag{9.15}$$

which, with the substitution $t/a_T = \theta$, becomes

$$G'(\omega;T) = \left\{\left[G_e(T_0)\right] + \omega a_T \int_0^\infty \left\{G(\theta;T_0) - \left[G_e(T_0)\right]\right\} \sin\omega \; a_T\theta \; d\theta\right\} / b_T \tag{9.16}$$

Comparison with Eq. 9.12 shows that this can be rewritten as

$$G'_r(\omega;T) = b_T G'(\omega;T) = G'(a_T\omega;\, T_0) = G'(\omega_r;\, T_0) \tag{9.17}$$

which represents time–temperature equivalence as it applies to the elastic modulus. The term reduced frequency ω_r, is used for $a_T\omega$ and reduced storage modulus $G_r(\omega;T)$ for $b_T G'(\omega;T)$. However, these notations are used differently by different authors that creates a confusion.

It is to be noted that the derivation of Eq. 9.17, in view of the limits of the integral in Eq. 9.12 requires that Eq. 9.11 be valid over the entire time scale, that is, the material be thermorheologically simple. This analysis can then be summarized as: if temperature superposition is valid for $G(t;T)$ for all t, it is also true for $G'(\omega;T)$ and indeed it is true for all ω.

The relationship expressing $G(t;T)$ in terms of $G'(\omega;T)$ also involves a Fourier sine transformation as

$$G(t;T) - \left[G_e(T)\right] = \frac{2}{\pi}\int_0^\infty \frac{G'(\omega;T) - \left[G_e(T)\right]}{\omega} \sin\omega t \; d\omega \tag{9.18}$$

One can therefore show the converse, that is, if temperature superposition is valid for the storage modulus $G'(\omega;T)$ for all ω, it is also true for the relaxation modulus $G(t;T)$ for all t.

Similarly, it can be shown that temperature reduction is valid for the loss modulus $G''(0;T)$ for all 0 if it is valid for $G(t;T)$ for all t; that is, if Eq. 9.11 is valid for all t, then

$$G''_r(\omega;T) = b_T G''(\omega;T) = G''(a_T\omega;\, T_0) = G''(\omega_r;\, T_0) \tag{9.19}$$

The previous equation is valid for all ω.
Similarly, for the creep compliance (J), it can be written as

$$J_r(t;T) = \frac{J(t;T)}{b_T} = J\left(\frac{t}{a_T}; T_0\right) = J(t_r; T_0) \tag{9.20}$$

9.5 SUPERPOSITION AND THE WILLIAMS–LANDEL–FERRY EQUATION

Another commonly used empirical equation for TTSP is the Williams–Landel–Ferry (WLF) equation. WLF equation is often used to construct master curve, which relates a shift in temperature with a shift in time. However, the equation has limited application to materials above the glass transition temperature. The WLF assumes that the fractional free volume of polymers increase linearly with temperature (Tschoegl et al., 2002), leading to the following form:

$$\ln a_T = \frac{-C_1(T - T_0)}{C_2 + (T - T_0)} \tag{9.21}$$

where C_1 and C_2 are the constants derived from curve fitting. The constants were assumed to be universal constants, independent of the polymer, provided that similar thermodynamic conditions exist inside the materials. In WLF equation, the standard temperature was considered as $T_s = T_g + 50$ K as reference temperature, for which the constants $C_1 = -17.44$ and $C_2 = 51.6$ were used. Later on, Ferry (1980) reported C_1 for rubbers ranging from -11 to -20 and C_2 varied between 25 and 108. The range of temperature for the application of the WLF equation is prescribed as $T_g < T < T_g + 100$ K, whereas some other authors recommended the same as $T_g < T < T_g + 150$ K.

Arrhenius (1889) suggested a time–temperature relation based on the concept of activation energy. The Arrhenius equation relates the rate constant k of chemical reactions to the temperature T and the activation energy E_a,

$$k = A\exp\left(-\frac{E_a}{RT}\right) \tag{9.22}$$

where R is the gas constant and A is a constant. Substituting the relaxation time τ for the reaction rate k, a shift factor can be derived in analogy to the WLF factor according to

$$\ln a_T = \frac{E_a}{R}\left(\frac{1}{T} - \frac{1}{T_{ref}}\right) \tag{9.23}$$

9.6 TIME–TEMPERATURE–STRESS SUPERPOSITION PRINCIPLE (LUO ET AL., 2012)

Since, higher temperatures and higher stress levels bring about an equal acceleration of creep deformation and shorten the relaxation time of the materials, there exists an analogy between time and stress, similar to the analogy between time and temperature described by TTSP. Stress plays an important role in the viscoelastic properties of materials similar to that of the temperature. A higher stress reduces the relaxation time of materials because of which the free volume of the material increases, and therefore, more void space is available for segmental mobility in polymers. It is assumed that the stress-induced change in the free volume fraction is linearly dependent on stress change, much like the effect of temperature on the change in free volume, and derived a temperature–stress shift factor $\phi_{T\sigma}$, which has the following form (Luo et al., 2001):

$$\log\phi_{T\sigma} = -C_1\left[\frac{C_3(T-T_0)+C_2(\sigma-\sigma_0)}{C_2C_3+C_3(T-T_0)+C_2(\sigma-\sigma_0)}\right] \tag{9.24}$$

where C_1, C_2, and C_3 are material parameters related to the reference temperature T_0 and stress σ_0. When $\sigma = \sigma_0$, Eq. 9.1 reduces to the WLF equation. If the measuring temperature and the reference temperature are same ($T = T_0$,), then the Eq. 9.1 reduced to the following form:

$$\log\phi_{\sigma} = -C_1\left[\frac{\sigma-\sigma_0}{C_3+(\sigma-\sigma_0)}\right] \tag{9.25}$$

This defines the stress shift factor and provides the TSSP.

Moreover, according to time–temperature–stress superposition principle, the stress shift factor at a definite temperature (ϕ_σ^T), the temperature shift factor at a definite stress level (ϕ_T^σ), and the temperature–stress shift factor ($\phi_{T\sigma}$) are interrelated in such a way that

$$\phi_{T\sigma} = \phi_T^{\sigma_0} + \phi_\sigma^T = \phi_\sigma^{T_0} + \phi_T^\sigma \tag{9.26}$$

Using these shift factors, the viscoelastic property functions, for example, the creep compliances, in different thermomechanical states will have an equal value but different time scales. This can be written as

$$D(T,\sigma,t) = D\left(T_0,\sigma,\frac{t}{\phi_T^\sigma}\right) = D\left(T,\sigma_0,\frac{t}{\phi_\sigma^T}\right) = D\left(T_0,\sigma_0,\frac{t}{\phi_{T\sigma}}\right) \tag{9.27}$$

Previous equations illustrate that the time-dependent mechanical properties of viscoelastic materials at different temperatures and stress levels for some convenient time scales can be shifted along the time axis to construct a master curve of a wider time scale at a reference temperature, T_0, and/or reference

stress level, σ_0. Furthermore, the master curve can be constructed by a single shift via the temperature–stress shift factor, $\phi_{T\sigma}$, or by pair-shift via a joint application of the time–stress shifting at specified temperature, ϕ_σ^T or $\phi_\sigma^{T_0}$, and the time–temperature shifting at specified stress level, $\phi_T^{\sigma_0}$ T or ϕ_T^σ. For more details readers can consult to the publication of Luo et al. (2012).

Similar to the TSSP, a TTSP approach which indicates that $D(T,t) = D\left(T_0, \frac{t}{\phi_T^\sigma}\right)$ is used to construct the master curve from the tests conducted at selected temperatures and a specified stress level.

9.7 CONSTRUCTING TTSP MASTER CURVE FOR DYNAMIC MODULI

The superposition of the response curves, by shifting along the log-(time) axis, to construct a master curve according to the TTSP, implies, within the context of the scaling properties, that the different curves must be related by scaling with a translation path parallel to the horizontal axis (Povolo and Fontelos, 1987).

Various steps for constructing a master curve for a particular rheological modulus are described next. The loss modulus (G'') and the complex viscosity (η^*) against frequency (ω) data have been used for the illustration.

1. A sample is subjected to frequency sweep measurement in a linear viscoelastic region (LVR). Determination of LVR is required before beginning frequency sweep test to confirm the stability of microstructure of the sample under shear environment. Construction of a master curve is illustrated in Fig. 9.2a (η^*–ω) with two set of isothermal studies carried out at temperature T_1 and T_2, respectively. Similarly, Fig. 9.3a illustrates the viscous modulus data of melt rheology of polylactides (PLAs) as function of frequency (G''–ω) at selected temperatures (170, 180, and 190°C).
2. A reference temperature is selected arbitrarily or based on a temperature of interest (eg, melting point). A reference temperature of T_1 and 180°C have been selected for constructing those master curves.
3. All the individual frequency curves at selected temperature levels are shifted along the frequency scale to construct a master curve. Two shift factors namely horizontal (a_T) and vertical (b_T) are required for the superimposition of those curves. Figs. 9.2b and 9.3b are plots of reduced η^* and G'' versus $a_T\omega$. Only inclusion of one shift factor a_T generates the master curve as in Fig. 9.3b, whereas both factors are used to construct Fig. 9.2b. The shift factors allow it to join smoothly into the master curve. For TCMs the viscoelastic properties do not superpose completely if only horizontal displacements are performed. Vertical shift factors are needed to account for change in material density, hygrological effects, and thermal expansion and contraction (Alwis and Burgoyne, 2008). Fig. 9.3c shows the shift factors as a function of temperature for PLA sample.

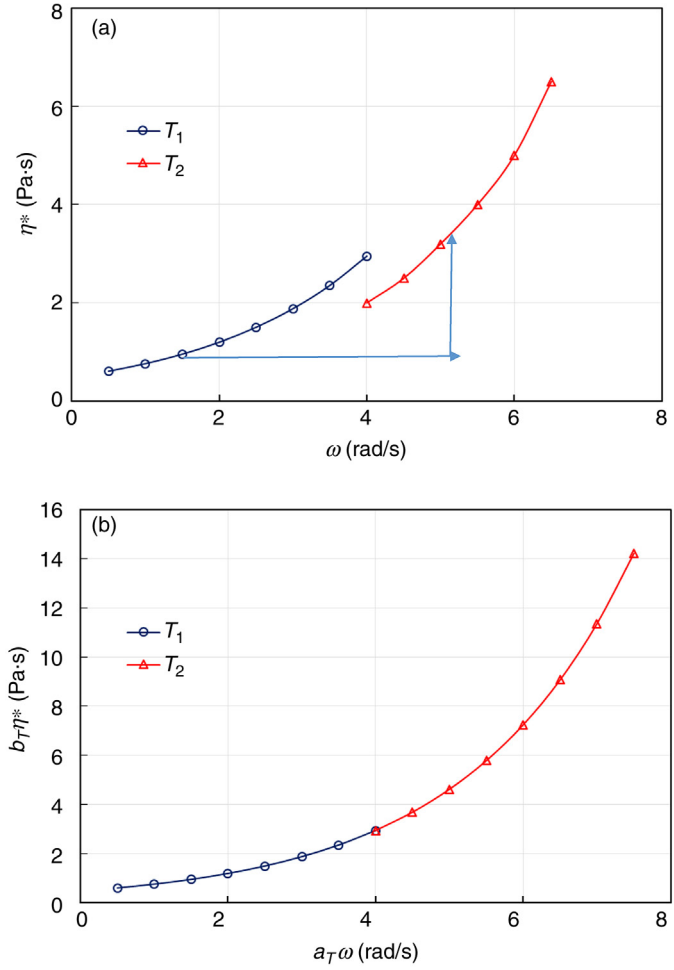

FIGURE 9.2 Construction of master curve from the individual isothermal studies. (a) Individual isothermal studies at temperature T1 and T2, (b) construction of master curve from two isothermal studies.

9.7.1 Some Other TTSP Approaches for Oscillatory Rheology

The analysis of TTSP applicability for different materials is also carried out by using a Cole–Cole plot [$E''(\omega)$ vs $E'(\omega)$ or $G''(\omega)$ vs $G'(\omega)$, at several temperatures]. When the behavior of the Cole–Cole plot is temperature independent, only horizontal shift is required and the material can be considered as thermorheologically simple. However, in many cases, it has been seen that the Cole–Cole plot is temperature dependent, that is, both horizontal and vertical shifts are required to apply the TTSP. A representative rheogram for polymer/

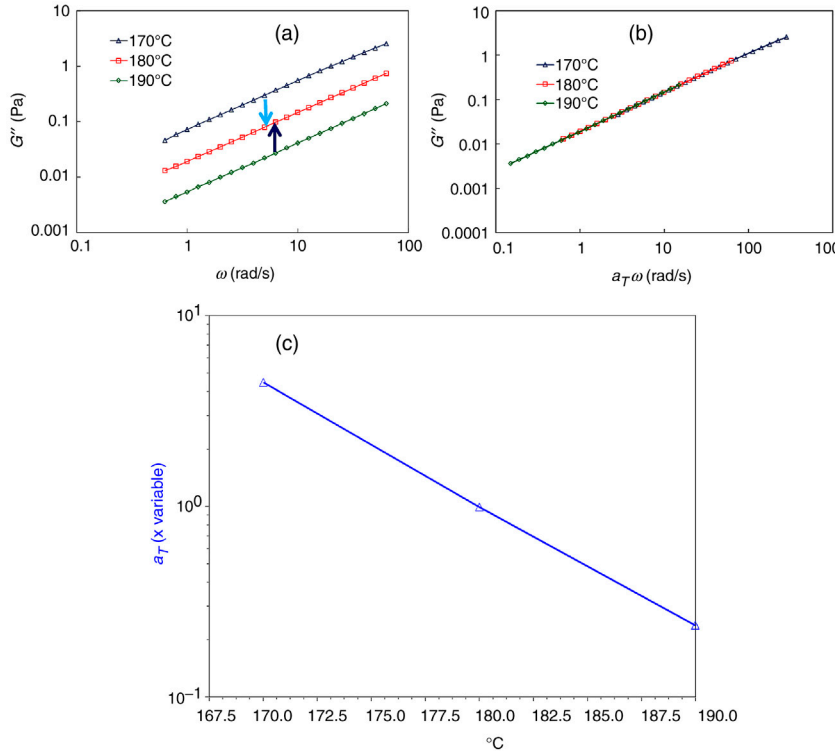

FIGURE 9.3 (a) Isothermal curves for a biopolymer (PLA) at selected temperatures, (b) TTSP curve with horizontal shift only, and (c) shift factors versus temperature.

nanoparticle composite is presented in Fig. 9.4a, where it is clearly observed that both shift factors have to be employed to generate a master curve.

It has been pointed out that the use of TTSP is meaningful as long as the morphology of the polymer remains the same over the range of temperature studied. Therefore, TTSP is very much unique for homopolymers. However, in recent years TTSP has been employed to compatible polymer blends on the basis of a single T_g, to microphase-separated block copolymers, and also to thermotropic liquid-crystalline polymers. To enhance the applicability of TTS, Han et al. (1983, 1986), Han (1988) advocated the use of log G' versus log G'' plots over log G'_r (or log G''_r) versus log ωa_T plots in obtaining temperature-independent correlations for polymer systems since log G' versus log G'' plots for homogeneous polymer systems are virtually independent of temperature. A typical modified Cole–Cole (MCC) plot is shown in Fig. 9.4c. The approach is in fact a modification of conventional Cole–Cole plot where the imaginary and real components of a complex modulus are plotted against each other on linear axes (Cole and Cole, 1941). Furthermore, those authors suggested that before attempting to apply TTSP to multicomponent and/or

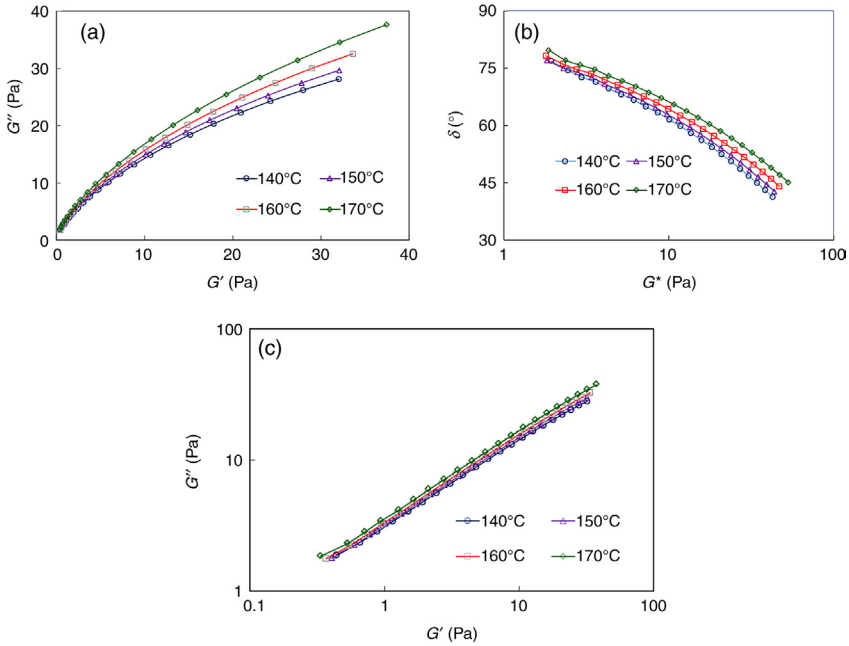

FIGURE 9.4 Applicability of (a) Cole–Cole plot, (b) van Gurp–Palmen (vGP) plot, and (c) modified Cole-Cole plot for polymer-based nanocomposite.

multiphase polymer systems, one must first observe whether or not plots of log G' versus log G'' show temperature independence. It has been observed that log G' versus log G'' plots are very sensitive to a variation in the morphological state of multicomponent/multiphase polymer systems (eg, immiscible blends, microphase-separated block copolymers, liquid-crystalline polymers), therefore, it has been pointed out that whereas the so-called Cole–Cole plot is strictly an empirical correlation, plots of log G' versus log G'' have a basis of molecular viscoelasticity theory and thus the two are not related to each other. In contrast to TTS, no data manipulation is required to superpose isothermal frequency (ITF) curves (Baek and Han, 1995). As temperature changes from T_1 to T_2, moduli automatically shift by the amount log $(T_1\rho_1/T_2\rho_2)$ (Han and Jhon, 1986; Han et al., 1989). Han and Kim (1993) deemed the MCC analysis as more sensitive than TTS, and readers can consult their original publication for further reading.

Another approach to obtain a TTS is the use of the vGP plot of phase angle (δ) versus complex modulus (G^*) to ascertain the thermorheological simplicity of a material. The VGP plot does not require a shift in frequency to a reference temperature to produce overlapping curves but only a shift in modulus with temperature (van Gurp and Palmen, 1998). The analysis of van Gurp and Palmen is a more accurate test for TTSP applicability. The measurements on LDPE/ZnO exhibit a distinct lack of overlap (Fig. 9.4b).

9.8 TTSP FOR CREEP BEHAVIOR

Based on the TTSP, the master curve of creep behavior against reduced time at a reference temperature is constructed by shifting the measured creep compliance (D_c) data at elevated temperatures along the log time axis (the horizontal axis). The measured creep data at higher temperatures cannot be superimposed smoothly by only horizontal shifting as shown in Fig. 9.5a. However, the smooth master curve may be obtained by shifting measured data horizontally as well vertically as illustrated in Fig. 9.5b. This vertical shifting is well known as the thermal correction based on the entropy elasticity at the temperature above T_g.

As shown in Fig. 9.6a, the D_c versus time curves measured at temperatures T_2 and T_3 are superposed onto that at T_1 by shifting D_c curves horizontally and vertically, to form a single master curve at a reference temperature T_0 (= T_1) against the reduced time t'. For more details, it is recommended to consult the publication of Nakada et al. (2011).

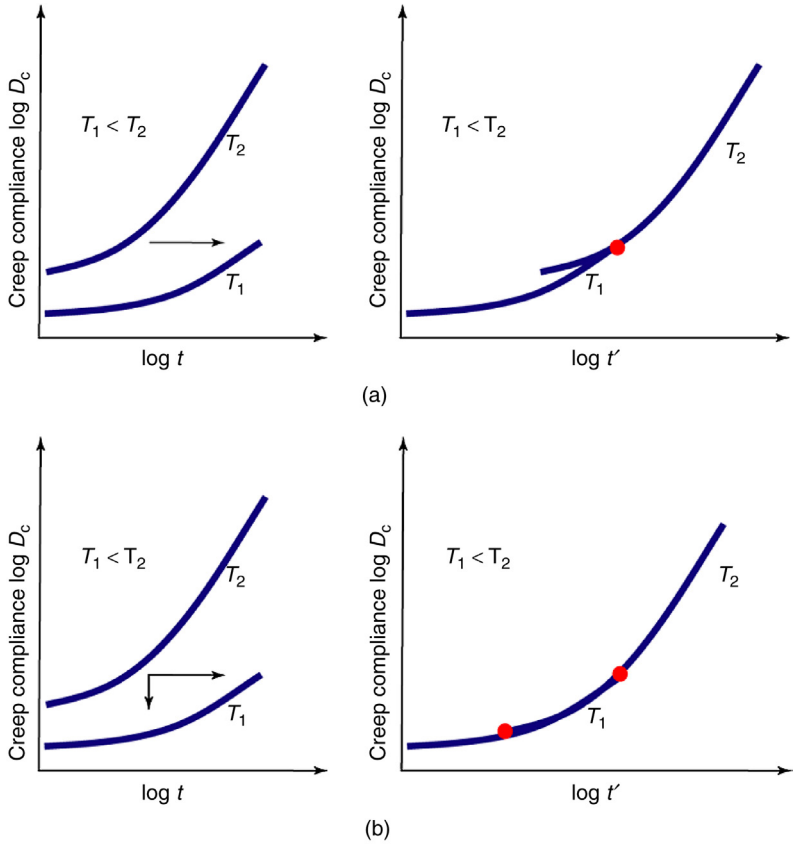

FIGURE 9.5 TTS for creep compliance. (a) TTSP (only horizontal shift) and (b) TTSP (horizontal and vertical shifts). *(From Nakada et al., 2011)*

The shift factors for those superposition $a_{T_0}(T)$ and $b_{T_0}(T)$ are defined by

$$a_{T_0}(T) = \frac{t}{t'} \tag{9.28}$$

$$b_{T_0}(T) = \frac{D_c(t, T)}{D_c(t', T_0)} \tag{9.29}$$

All the steps are similar as discussed earlier for dynamic moduli. The variation of the creep of the specimen is observed against the log (time), as illustrated in Fig. 9.6.

The most important consideration for such superposition is the smoothness where two different curves merge. If the TTSP method is valid, the master curve represents the true behavior of a long-term test at the reference temperature. That curve would be expected to be smooth, so it is a necessary condition that the master curve produced should also be smooth.

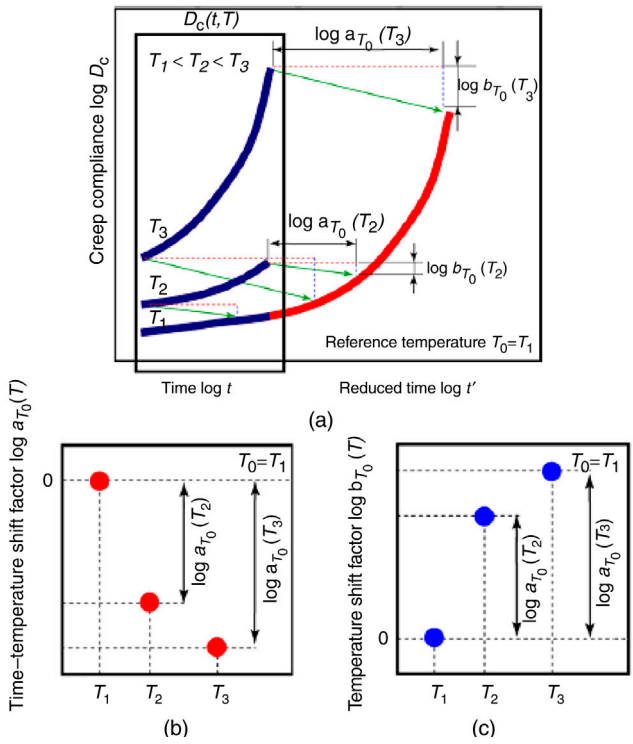

FIGURE 9.6 Master curves construction with creep compliance and effect of temperature on shift factors. (a) Master curve of creep compliance, (b) time–temperature shift factor, and (c) temperature shift factor. *(Adapted from Nakada et al., 2011)*

The accuracy of the master curve in a creep experiment depends on the following factors as suggested by Alwis and Burgoyne (2008):

1. Variation of the shift factors with temperature.
2. Retention of the same creep mechanism under studied temperatures.
3. The initial strain rate applied to a sample during the creep test. Although the creep stress, σ_0 is assumed to be applied instantaneously, a finite time and a certain rate of strain are desirable to attain the required stress level.
4. Change of humidity.
5. State of the material property (glassy, rubbery, or at the transition range).
6. Preparation of the specimens, the type of the clamping system, and the type of the testing machine.
7. Rate of heating to achieve an isothermal condition.

9.9 CONSTRUCTING MASTER CURVE BASED ON THE WLF EQUATION

Mostly, the mean a_T values are determined from both the dynamic moduli ITF data by fitting the WLF equation. Initially, the mean a_T values are calculated by linear regression analysis, and determined the WLF constants, C_1 and C_2, respectively. The master curve is generated by plotting moduli corrected for thermal expansion versus ωa_T on logarithmic axes by putting new a_T values obtained from C_1 and C_2. Nickerson et al. (2004) calculated mean a_T values for gellan in the presence of 80% (w/w) cosolutes by linear regression analysis, and determined the WLF constants, C_1 and C_2 to be 8.9 and 141.1 K, respectively. Using these constants, new a_T values were calculated, and presented in Table 9.1 which were used thereafter, to form a single master curve (Figs. 9.7 and 9.8).

9.10 FAILURE OF TTS CURVES (WOIRGARD ET AL., 1977)

In practice there are many reasons for the failure of TTSP. Important points are as follows:

- Temperature variation can cause structural changes in the specimen especially at the vicinity of the glass transition temperature.
- Phase transition can occur during the temperature scans. In composite materials, each constituent may have a different sensitivity to temperature.
- Viscoelastic spectra cannot be obtained by temperature scans if diffusion is active in the material.
- The theory of viscoelasticity holds under isothermal conditions and is not directly applicable if temperature is varied continuously.

TTS is not a definitive test to check linearity in material behavior, that is, a linear viscoelastic material may or may not obey TTS (Lakes, 2004).

TABLE 9.1 TTS Shift Factors (a_T) (Logarithmic) as a Function of Temperature (85–15°C) During Cooling for a 0.5% (w/w) Gellan:80% (w/w) Cosolute Sample

Temperature (°C)	Log a_T (G')	Log a_T (G'')	Mean log a_T	Calculated log a_T
85	−2.00	−2.00	−2.00	−1.95
75	−1.53	−1.52	−1.52	−1.55
65	−1.10	−1.10	−1.10	−1.10
55	−0.60	−0.57	−0.59	−0.59
45	0	0	0	0
35	0.65	0.70	0.68	0.69
25	1.48	1.48	1.48	1.50
15	2.40	2.40	2.40	2.46

Shift factors were obtained by shifting ITF data for G' and G'' to allow curves to superimpose. Mean log a_T values were used to determine the WLF constants, which were then fitted with the WLF equation to calculate log a_T values required to form the master curves.
Source: Adapted from Nickerson et al. (2004)

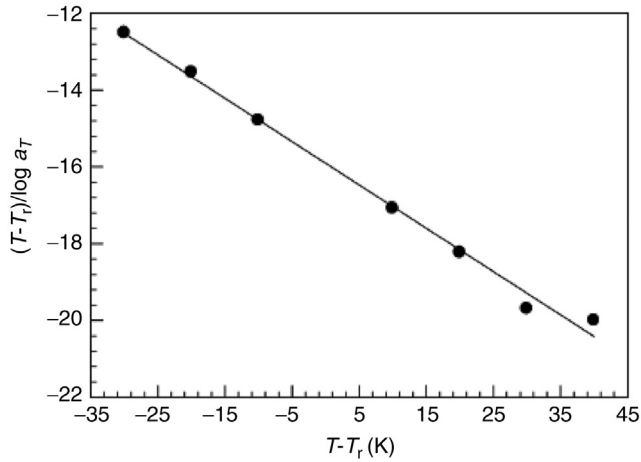

FIGURE 9.7 TTSP shift factors fitted with the WLF equation for a 0.5% (w/w) gellan, 80% (w/w) cosolute sample at a reference temperature of 45°C. *(Adapted from Nickerson et al., 2004)*

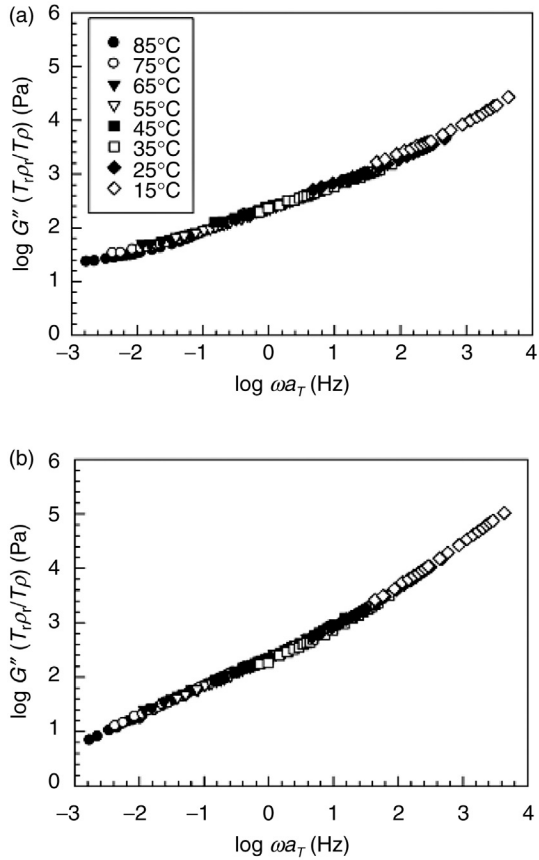

FIGURE 9.8 TTSP master curves for G' (a) and G'' (b) for a 0.5% (w/w) gellan, 80% (w/w) cosolute sample during cooling at a reference temperature of 45°C. *(Adapted from Nickerson et al., 2004)*

9.11 APPLICATIONS

9.11.1 Nanocomposites

TTS is frequently used for nanocomposites although there have been mixed opinions on the application of TTS to nanocomposites. Solomon et al. (2001) applied the concept to melt-compounded polypropylene filled with organophilic nanoclay in the presence of a compatibilizer, and they found a similar temperature dependence of shift factors in the nanocomposites as in the neat polymer. The application of TTSP was successful with extruded and injection-molded polypropylene filled with organophilic layered silicates that were annealed (Reichert et al., 2001). They used the shifting procedure as a tool for the investigation of clay platelet network formation and observed that the annealing

process improves exfoliation and facilitates the formation of a thermodynamically stable structure. Application of TTS to some polymeric nanocomposites indicated that the TTSP is valid with a limited range of temperature. For poly(butylene terephthalate)/MWCNT nanocomposites the TTSP followed only in a narrow range of temperature 230–240°C, and the principle failed above 260°C (Wu et al., 2007). It is believed that the successful superposition at higher reduced frequencies is due to dominant local chain dynamics, and the failure of superposition at lower reduced frequencies is influenced by the different temperature dependence of the percolated network. None of the reported studies attempted any application of vertical shifting.

Ahmed et al. (2010) constructed the linear viscoelastic master curves for the pure PLA melt (184–196°C) using the TTSP at a reference temperature of 190°C. Both the shift factors a_T and b_T were used to generate a master curve. Fig. 9.9 illustrates the reduced angular frequency dependence of the dynamic moduli (G', G'', and η^*) for the neat PLA specimens at selected temperatures (184, 187, 190, 193, and 196°C). Samples experiencing a short thermal history (corresponding to high frequencies: 1–10 Hz) produce a satisfactory

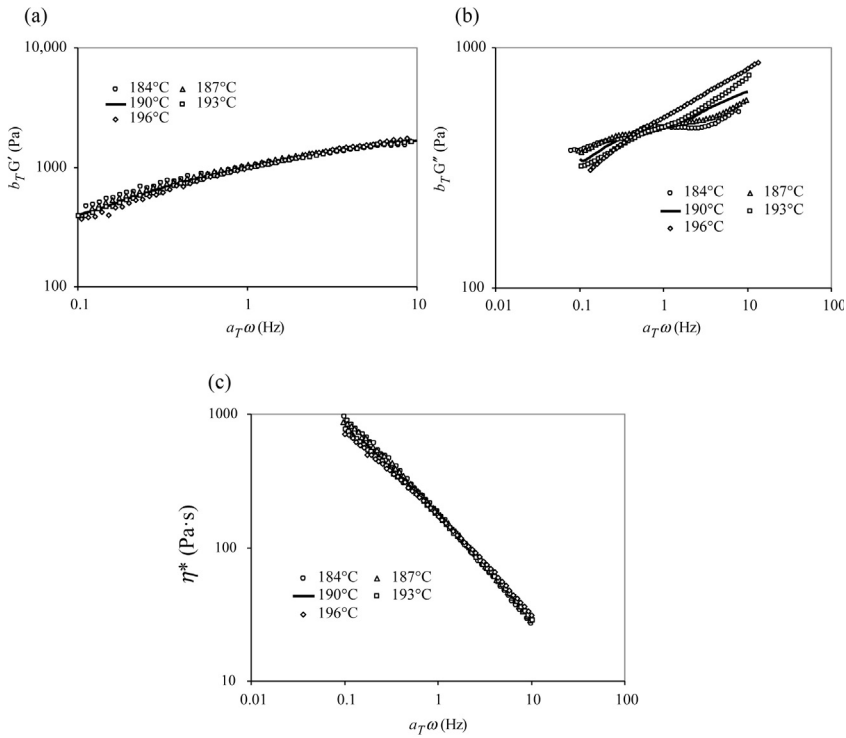

FIGURE 9.9 Reduced angular frequency dependence of mechanical spectra (a) elastic modulus (G'), (b) viscous modulus (G''), and (c) complex viscosity (η^*) for neat PLA specimens at selected temperatures. *(Adapted from Ahmed et al., 2010)*

overlapping of the curves. However, longer thermal exposure (0.1–1 Hz) produces significant deviations from the TTS (especially G'') due to ongoing chemical degradation (Palade et al., 1995). In addition, it was observed that the highest temperature (196°C) showed the maximum deviation from the superposition which is very common for rapid chemical degradation at higher temperatures. The deviation of complex viscosity at 196°C is obvious in higher frequency range too (Fig. 9.9c).

TTSP was employed to obtain creep deformation of the plasticized starch/cellulose nanofibrils (5–20% wt/wt) and plasticized starch–only films in longer time frame (Meng et al., 2015). The creep for both types of films were measured at six selected temperatures (30, 35, 40, 45, 50, and 55°C) at a static stress of 8 MPa for 5 min. All the individual creep curves obtained at different temperatures were shifted to a reference temperature of 55°C along the logarithmic time axis to superimpose to a master curve. The temperature dependence of the shift factors showed a good linear relationship with the absolute temperature.

Yang et al. (2015) developed a master curve of creep compliance (S) as a function of temperature (20–50°C in an interval of 5°C) and time, and the activation energy of the glass transition relaxation of bamboo fiber–reinforced recycled PLA composites by DMA. In the work, the reduced time using a shift factor (αT) was calculated from TTSP, and, thereafter, the creep curves at elevated temperatures were shifted along the time axis toward the right. Arrhenius equation was used for calculating the activation energy from the shift factors of the NC. The E_a values were in the range of 428.5–493.2 kJ/mol. Furthermore, the creep compliance master curves of the various bamboo fiber–reinforced recycled PLA composites were generated using shift factors, and estimated from a constant activation energy assumption. The master curves were modeled with the Findley power law, which is presented in the following equation:

$$S(t) = S_0 + a\ t^b \tag{9.30}$$

where $S(t)$ is the time-dependent compliance, S_0 is the instantaneous elastic compliance, a and b are constant numbers, and t is the elapsed time.

Several researchers attempted to shift the frequency dependence of viscoelastic moduli of polymer/nanoparticles measured at selected temperatures, and observed that the data superposed unsatisfactorily. Handge and Pötschke (2007) worked on polycarbonate/MWCNTs (2 wt.%) at 190 and 210°C, and they suggested that the failure of TTS implied that the relaxation processes of the pure polymer and filler network had different temperature dependence, and they attributed the influence of interactions between the polymer and filler more to entropy elasticity of the melt than to temperature. Similarly, Wu et al. (2007) concluded that TTS was possible in poly(butylene terephthalate)/MWCNT nanocomposites in a narrow temperature window of 230–240°C, but not at higher temperatures up to 260°C. They attributed the successful superposition at higher reduced frequencies to dominant local chain dynamics and the failure

of superposition at lower reduced frequencies to the different temperature dependence of the percolated network.

TTSP was applied to produce the master curves of the dynamic moduli obtained for a PLA/nanographite platelets (1–10 wt.%) nanocomposites melt (170–200°C) at a reference temperature of 180°C (Narimissa et al., 2014). The master curves of G' and G'' showed that the change in liquid-like behavior into pseudosolid-like behavior occurred at 3 wt.% nanographite platelets content in the composites. The complex viscosity master curves indicated that a change from Newtonian to shear-thinning behavior at low frequency region occurred at 5 wt.% filler content.

Applicability of TTSP for a nanocomposite based on poly(ε-caprolactone) (PCL) and organomodified clays (Cloisite 30B and Cloisite 15A) (PLANC) were studied (Ahmed et al., 2012; Nikolic et al., 2016). The linear viscoelastic master curves for the PCLNC are generated at selected temperature range (90–120°C) by the TTSP and shifted to a reference temperature of 100°C employing both shift factors (Ahmed et al., 2012). Samples experiencing a short thermal history (1–10 Hz) produce a satisfactory overlapping of the curves, whereas, longer thermal exposure (0.1–1 Hz) produces deviations from the TTSP (especially G' at 10% clay). Furthermore, the deviation was obvious at higher temperature (110–120°C) because of rapid chemical degradation at higher temperatures. This observation is supported by shift factors at various clay concentrations, which are reported in Table 9.2. Han plots were employed to detect the possible structural changes with temperature. Nikolic et al. (2016) reported that no microstructural changes occur for the studied nanocomposites within the studied temperature range except for the NC loaded with 8% C15A clay. Such changes in the nanocomposite structure have been explained by the dynamic percolation structure or by the enhanced dispersion of the clay induced by temperature changes during the tests. Applied frequency shift factors are relatively small and comparable to reported values for pure PCL and its various nanocomposites in the similar temperature regime. The shift factors used to obtain good superposition for the nanocomposites seem to be independent of the clay loading. The independence of shift factors on the type and the amount of clay, as previously observed, indicate that the relaxation processes taking place in the nanocomposites originate from the unaltered polymer matrix.

Another approach known as van Gurp–Palmen (vGP) plot (van Gurp and Palmen, 1998) has also been used to verify the TTSP in polymer blends and nanocomposites. The vGP plot as a typical dependency of loss angle δ on complex modulus $|G^*|$ has been used in order to evaluate the topological structures of polymers (Kracalik et al., 2011). The novelty of this plot is that there is no need of shift factor along the frequency axis for superposition of curves. The vGP plot for PCLNC, PCL, and its nanocomposites are illustrated in Fig. 9.10.

It can be seen that the δ decreased with increasing G^*, and increased furthermore irrespective of the processing temperature. However, rheograms are almost superimposed except at 90°C indicating insignificant change in the

TABLE 9.2 Shift Factors for Applicability of TTSP for PCL/Clay Nanocomposite at Selected Clay Concentrations

Temperature (°C)	TTSP for G'						TTSP for G''					
	5% NC		7.5% NC		10% NC		5% NC		7.5% NC		10% NC	
	a_T	b_T	a_T	b_T	a_T	b_T	a_T	b_T	a_T	b_T	a_T	b_T
90	0.88	1.01	1.07	1.01	1.00	1.01	0.84	1.01	1.06	1.01	1.06	1.01
95	0.97	1.01	1.00	1.01	0.98	1.01	0.96	1.01	1.00	1.01	1.01	1.01
100	1.00	1.00	1.00	1.00	1.00	1.00	1.00	1.00	1.00	1.00	1.00	1.00
105	1.00	0.99	0.89	0.99	0.96	0.99	1.01	0.99	0.91	0.99	0.96	0.99
110	0.96	0.99	0.79	0.99	0.93	0.99	0.99	0.99	0.83	0.99	0.91	0.99
120	0.87	0.98	0.65	0.99	0.83	0.98	0.92	0.98	0.71	0.98	0.82	0.98

Source: Adapted from Ahmed et al. (2012)

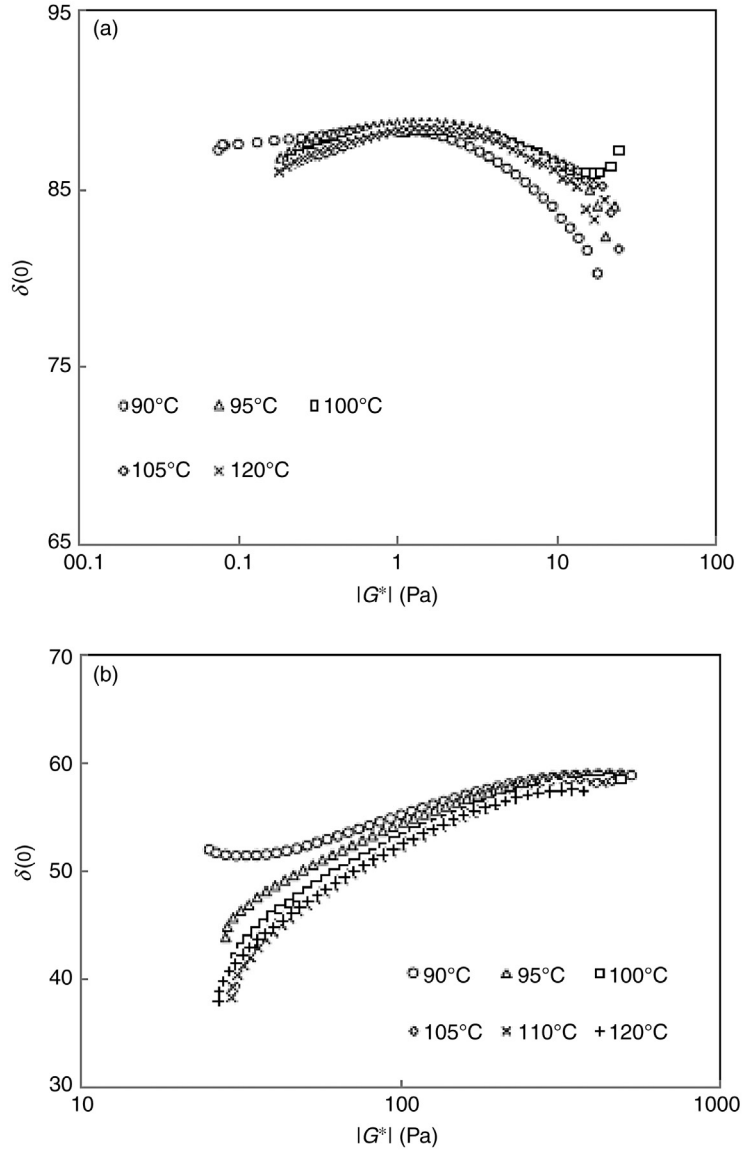

FIGURE 9.10 Phase angle versus absolute complex modulus (vGP plot) of (a) PCL and (b) 10% clay incorporated PCLNC as a function of processing temperature. *(Adapted from Ahmed et al., 2012)*

polymer structure. For the nanocomposite films, an interesting behavior of the δ versus G^* curves was observed (Fig. 9.10b). The phase angle decreased significantly for all clay loading at similar temperature regime. Furthermore, there is a significant shift in the δ versus G^* curves at selected temperature, especially a lower G^* value. As the temperature is raised, the contribution of the polymer matrix decreases and the solid-like behavior of the nanofiller network dominates the rheological response of the nanocomposite film. Thus, the shift is a clear indication of the change in nanofiller dispersion with changing processing temperature. It further indicates that TTS does not fit well for clay-incorporated PCLNC.

9.11.2 Polysaccharide/Sugar Mixtures

Time–temperature studies of polysaccharide gelation allow macrostructure changes to be studied as a function of temperature and frequency as reported by Nickerson et al. (2007). Authors studied changes to dynamic moduli (G' and G'') as a function of temperature and oscillatory frequency for 0.5% (w/w) gellan/80% (w/w) cosolute dispersions with added Na^+ (40–160 mM). ITF (0.15–15 Hz) and thermal scans at 0.15 Hz were performed over a decreasing and increasing temperature range of 85–5 and 5–85°C, respectively. ITF data were described using TTSP and MCC analysis.

At 40-mM Na^+ level, the ITF data during cooling/heating were superposed well over the entire temperature range for both moduli, except at 5°C. Authors believed that deviations of the oscillatory frequency data at 5°C from the master curve occur from errors within the data transformation rather than the TTS failure. Furthermore, these errors reflect differences between experimental and calculated a_T values used by the WLF equation, which become magnified by the logarithmic transformation during the application of the method of reduced variables. However, the MCC analysis required no data transformation to superpose the 5°C oscillatory frequency data within the master curve. Therefore, the MCC analysis was presumed to validate the success of TTS over this temperature range. Successful superposition suggests that the material behaved as a thermorheologically simple material where no changes in relaxation mechanisms occurred with temperature. Additionally, the viscoelastic response was dominated by the long-range relaxation of gellan chains between junction zones.

The gellan/high cosolute samples with 100-mM Na^+ showed different rheological behavior during heating/cooling. During cooling, the sample exhibited a thermorheologically complex behavior and the ITF data failed to superpose. However, the sample superimposed completely during heating over the complete temperature range, and exhibited a thermorheologically simple material. The lack of superposition of the 5°C ITF is analogous to the 40-mM Na^+ sample, which was considered to be successfully superposed. The crosslinked network formed after cooling is thought to be again weakly associated since junction zones were not temperature dependent. With the addition of 160-mM Na^+, TTS

failed at all temperatures during both cooling and heating due to the formation of ion-mediated junction zones of sufficient number and size to dominate the viscoelastic response of the material over the entire temperature range.

9.11.3 Pectin

The rheological parameters obtained in the temperature range of 5–65°C for the high-methoxyl pectin and low-methoxyl pectin dispersions in water (3.5%, w/w) and in 0.1 M NaCl were reduced to a reference temperature of 25°C, using the TTSP (da Silva et al., 1994). Both the G' and the G'' data as a function of frequency were first plotted using modulus shift factors calculated from the temperature/density correction factor ($T_0\rho_0/T\rho$). Then, the appropriate a_T was obtained empirically by graphical shift of the data obtained at different temperatures, using logarithmic ordinates. Over the entire temperature and frequency range, the TTSP could not be applied to simultaneous superposition of $G'(\omega)$ and $G''(\omega)$ data. Furthermore, satisfactory reduction of the data to a single master curve was not obtained, irrespective of the frequency shift factor employed, for each modulus individually or with vertical shift factors higher than those calculated by the temperature–density factor. For the steady shear data $\eta(\gamma)$ obtained by decreasing applied stress, after shearing the sample, satisfactory superposition could be obtained only by applying b_T higher than those obtained by the temperature–density factors.

The failure of the TTSP to be applied to pectin dispersions, in the range of temperature studied, could be attributed to structural changes in the pectin aggregates resulting from temperature changes that in turn affected the chain mobility on which the rates of all configurational rearrangements depend. The higher values of the shift factors of pectin samples, are the result of greater temperature sensitivity of the intermolecular interactions taking place in these systems.

9.11.4 Mung Bean Starch

The applicability of TTSP has been tested for legume starch dispersions. Ahmed (2012) employed TTSP for mung bean starch individually and blended with salt and sugar (5–10% w/w) in dispersions. The ITF sweep tests were conducted at selected temperatures (70–90°C), and shifted to a reference temperature of 80°C. Both the horizontal and vertical shift factors were employed for the superposition. The superposition of G'–ω data for starch dispersion was not satisfactory as can be seen from Fig. 9.10a, whereas a plot of η^* versus ω showed a better superposition at a reference temperature (Fig. 9.10b) except for 95°C. The nonapplicability of TTSP was pronounced at two extreme temperatures namely 70 and 95°C. It has been reported that the applicability of TTS should be examined above the glass transition temperature, and that could be the reason for nonapplicability of TTSP at 70°C, which is at the vicinity of T_g. Furthermore, the deviation above 85°C is believed to be associated with leaching of amylose and breakdown of amylopectin at high temperature.

TTS for 5% NaCl-incorporated starch blend fitted well and scaling has minimum effect on extending the frequency window (Fig. 9.11a). The shift factor values ranged within unity for all studied temperature range except at 85°C (a_T = 0.89). A better superposition at 5% NaCl loading concentrations might be attributed to salting-out effects, which will enhance the aggregation of amylose chains and the formation of a three-dimensional network (Ahmad and Williams, 1999). However, a further increment of salt level to 10% failed the

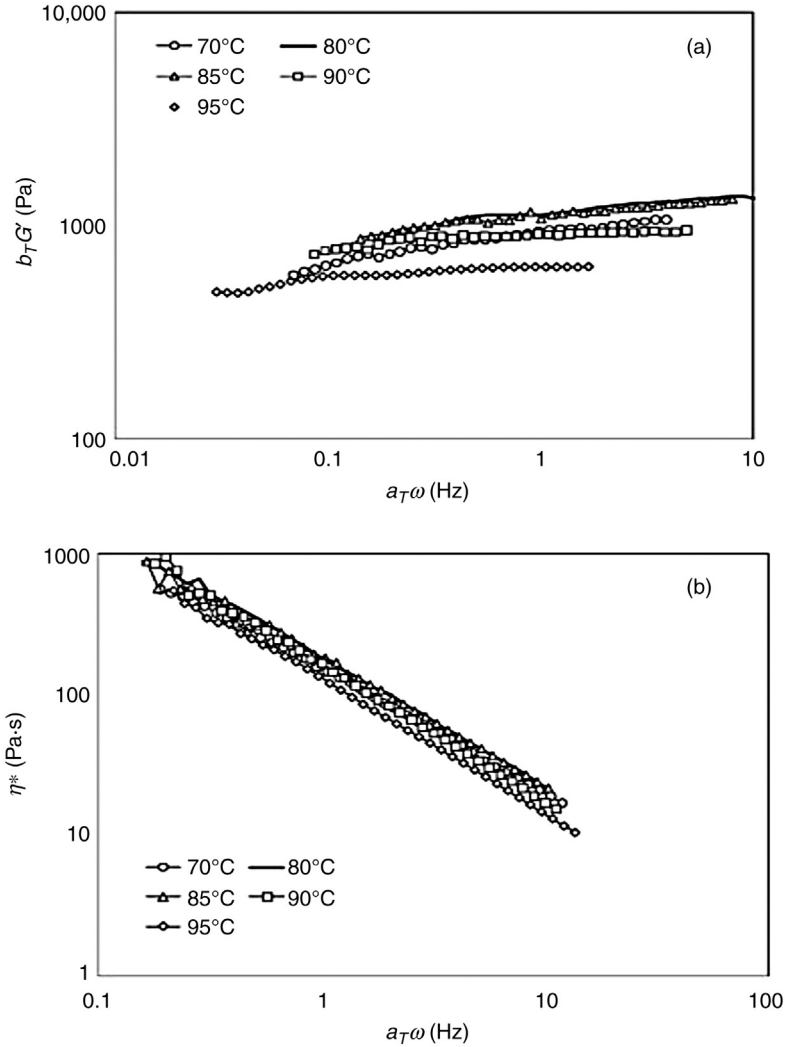

FIGURE 9.11 Master curves of (a) dynamic modulus and (b) complex viscosity versus frequency for mung bean starch dispersion (1:3 starch to water) to a reference temperature of 80°C. *(Adapted from Ahmed, 2012)*

TTSP at the reference temperature (Fig. 9.11b). Interestingly, isothermal heating at and above 85°C showed a superposition for salt-incorporated starch samples, and a new master curve was generated. The newly generated master curve exhibited better superposition (a_T values were very close to unity for 85–95°C).

Incorporation of sugar into starch matrix behaves differently compared to salt/starch blend (Fig. 9.12). A loading of 10% sucrose to starch shows a better superposition than 5% sucrose. Extending of frequency window was small

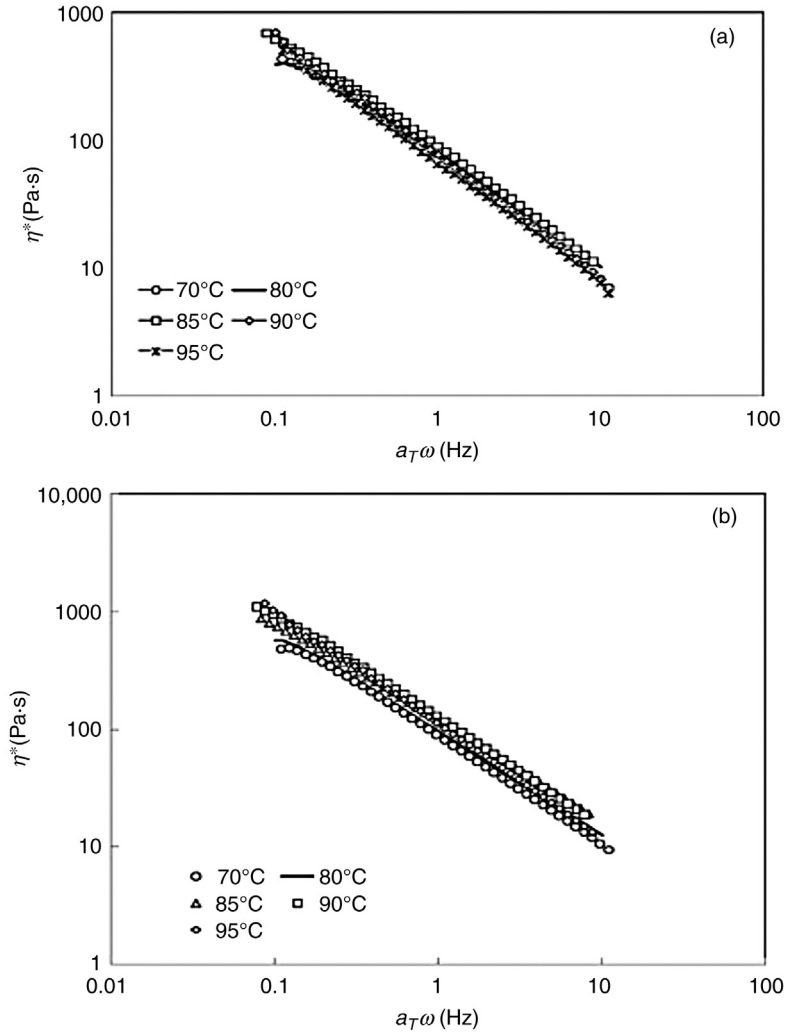

FIGURE 9.12 Reduced frequency dependence of complex viscosity of sodium chloride-added mung starch gel at reference temperature of 80°C. (a) 5% and (b) 10%. *(Adapted from Ahmed, 2012)*

for 10% sucrose because values of scaling coefficient a_T were close to unity except at 95°C (Fig. 9.12b). The applicability and nonapplicability of TTS to a blend system like salt and sugar indicates about internal stability of created structure in analyzed range of temperatures. These observations indicated that starch–sucrose–water matrix is very complex in nature. The difference in additives' effectiveness can be attributed to the penetration of the solute into the granule interior. Such penetration produced disorder inside the starch granules (Fig. 9.13).

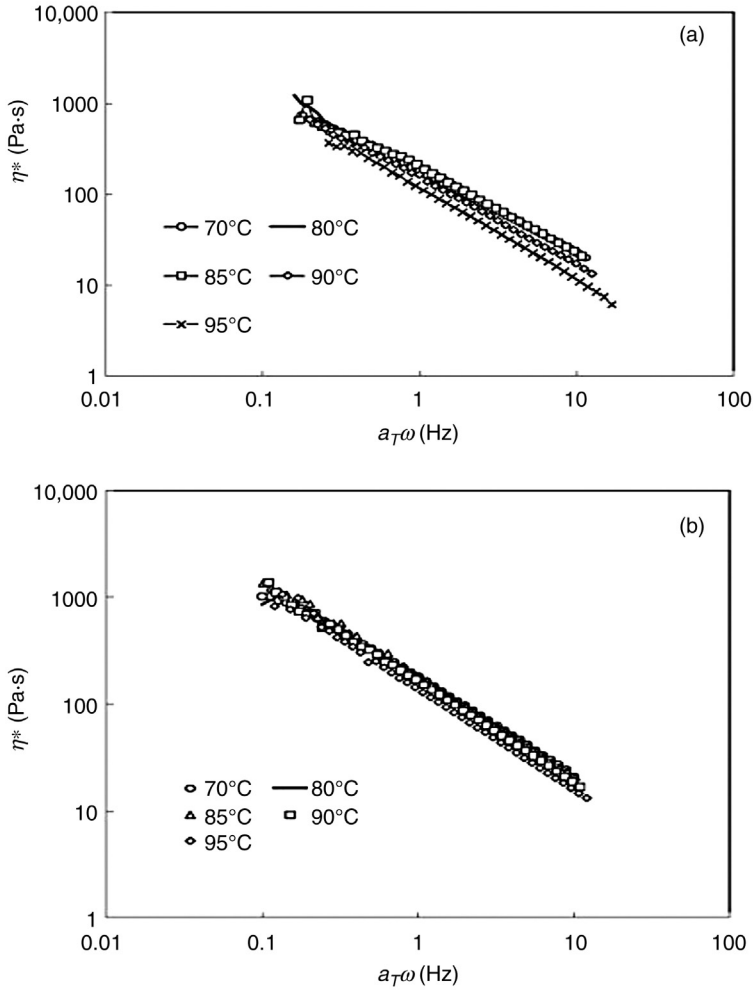

FIGURE 9.13 Reduced frequency dependence of complex viscosity of sucrose-added mung starch gel at reference temperature of 80°C. (a) 5% and (b) 10%. *(Adapted from Ahmed, 2012)*

9.11.5 β-Glucan Concentrate–Enriched Wheat Flour Dough

The linear viscoelastic master curves for the β-glucan concentrate–enriched wheat flour dough samples are generated by the TTSP. Rheological measurements were carried out at five selected temperatures (25, 40, 55, 70, and 85°C), and shifted to a reference temperature of 55°C using both the shift factors (Ahmed, 2015). The reference temperature is selected based on the dough softening temperature. A plot of the reduced angular frequency, $a_T\omega$ against the elastic modulus (G') and the complex viscosity (η^*) of the dough samples indicated that the η^* produced a good superposition whereas the G'–ω failed to follow superposition adequately, especially at the highest temperature employed (85°C). This observation clearly indicated that the mechanical rigidity generated on the dough samples during isothermal heating at 85°C was completely different from those at other temperature regimes. One of the best reasons for the nonapplicability of TTS for G'–ω could be the temperature range which are at extremes from the thermal transition of the dough. The shift factors also indicate that the starch/protein of the dough is strongly temperature dependent.

9.11.6 Cheese

Singh et al. (2006) studied the applicability of TTS for mozzarella cheese at selected temperatures (2, 10, 22, 30, 40, 50, and 60°C) and found that the amount of overlap for dynamic data at different temperatures reduced with increase in temperature. The curves at temperatures of 40 and 50°C show less overlap, as compared to the curves at 2 and 30°C. It concludes that cheese can be classified as TCM in the tested frequency range. However, this observation is in contrast with earlier reports on low-moisture part-skim mozzarella cheese (Subramaninan and Gunasekaran, 1997) where the dynamic data at different temperatures overlapped sufficiently to follow TTS in the frequency range of less than three decades. The heterogeneous nature of cheese, where each phase (fat, protein, and serum) can have its own temperature-dependent material properties, can make it thermorheologically complex.

The application of TTS and Cole–Cole analyses, were evaluated on the rheological data obtained for various types of cheeses. Various authors (Udyarajan et al., 2007; Meza et al., 2012) reported that cheeses exhibited deviation from TTS. Udyarajan et al. (2007) compared rheological behavior during heating/cooling period and noted that during the heating cycle, cheese samples (part-skim and fat-free) exhibited thermorheologically complex behavior. This complex behavior was probably because of the interaction of newly formed insoluble Ca^{++} at high temperature with caseins. During cooling cycle, cheeses appeared to obey TTS, indicating a thermorheologically simple behavior. Both part-skim mozzarella and fat-free cheese deviated from the type of behavior expected for a single Maxwell element in Cole–Cole analyses. Meza et al. (2012) employed TTSP and MCC analysis for comparison studies on cheeses (seven commercial

TABLE 9.3 Values of Shift Factors (a_T) as a Function of Temperature for Frozen and Refrigerated Commercial Low-Fat Soft Cheeses Containing Microparticulated Whey Proteins as Fat Replacer

Samples	Temperature (°C)	Log a_T (G'')	Log a_T (G')	Mean log a_T
Frozen cheeses	10	0.3	0.3	0.3
20	0	0	0	
30	−1.70	−1.70	−1.70	
40	−2.10	−2.70	−2.40	
50	−2.70	−3.70	−3.20	
Refrigerated cheeses	10	0.78	0.78	0.78
20	0	0	0	
30	−1.22	−1.22	−1.22	
40	−2.40	−3.40	−2.90	
50	−3.22	−4.70	−3.96	

Source: Adapted from Meza et al. (2012)

low-fat soft cheeses incorporated with microparticulated whey proteins as fat replacer) stored at refrigerated (6°C) and frozen (−25°C) storage. The results obtained in this work indicated that the viscoelastic properties of the studied cheeses obtained at different temperatures were influenced by freezing. Frequency sweeps (0.01–10 Hz) were carried out at 10–50°C with an increment of 10°C at a fixed stress amplitude (318 Pa). Values of a_T as a function of temperature for frozen and refrigerated cheeses are shown in Table 9.3. A satisfactory application of the TTS suggests that the material is thermorheologically simple, where relaxation times for all mechanisms change in the same way with temperature. In this study, superposition of ITF data gave similar a_T values at low temperatures (10–30°C) for both G' and G'' (Table 9.3). This result indicates that, in low-temperature region, both frozen and refrigerated cheeses behave like a thermorheologically simple material. However, superposition of ITF data did not give similar a_T values at high temperatures (40–50°C) for both G' and G''. The high-temperature data exhibited slight deviation from the TTS in master curves of G' and G'' when mean values of a_T were used to superimpose moduli. Muliawan and Hatzikiriakos (2007) indicated that, at temperatures higher than 40°C, mozzarella cheese started to melt undergoing structural changes. For those authors, viscoelastic data showed that cheese behaved as a physically different material depending on temperature.

MCC plots for frozen and refrigerated cheeses indicated that both elastic and viscous moduli could be superimposed at temperatures between 10 and 30°C. However, moduli failed to superpose at temperatures higher than 30°C, indicating temperature-dependent morphological changes in the cheese matrix. The MCC further supported the results obtained by the application of the TTS. Therefore, in the temperature range between 10 and 30°C, both moduli displayed similar temperature dependence, allowing successful superposition with both TTS and MCC.

9.11.7 Juice Products

TTSP has been used to model the effect of temperatures (6–75°C) and concentrations (20–50°Brix) on the rheological behavior of pummelo juice concentrates (Chin et al., 2009). To obtain an overall picture of the flow behavior of pummelo juice concentrate, the master-curve technique was used to model the rheological behavior to obtain a general fluid characterization irrespective of its temperature. The master-curve was generated by determining the shift factor, a_T with a reference temperature of 20 °C and a shear stress of 2.5 Pa. A plot of original shear stress in *y*-axis against the shifted shear rates in *x*-axis divided by the shift factors in logarithmic scales yielded a linear line for each concentration due to the horizontal shifting of data which caused an overlap.

Quek et al. (2013) combined a total of 35 average flow curves of soursop juice concentrates at 7 different temperatures (10–70°C) and 5 different concentrations (10–50°B) for generating a master curve at a reference temperature of 50°C and a reference shear stress of 1 Pa. Authors used two steps of shifting: one for the temperature and the second one for concentration. The master curve was then plotted as shear stress versus shear rate divided by the dimensionless shift factor $\left(\dot{\gamma} / a_T\right)$. The horizontal shifting with a_T combined the seven temperatures to overlap on one master curve for each concentration. Power law equation was then fitted to the five concentration master curves to obtain the expression of rheological behavior of soursop juice concentrates in terms of consistency coefficient, K' and flow behavior index, n'.

In the second shifting step, concentration master curves were moved to a reference concentration of 30°Brix at a shear stress of 1 Pa to construct a single master curve using the concentration shift factor of a_C and the second reduced shear rate, is quantified as $\dot{\gamma} / (a_T / a_C)$. The final master curve was plotted as shear stress versus shear rate divided by the dimensionless temperature shift factor and concentration shift factor to estimate the rheological behavior of soursop juice concentrates at concentration of 10–50°Brix and temperature of 10–70°C. The final master curve was also fitted to the Power law equation to obtain a single expression of rheological behavior of soursop juice concentrates in terms of consistency coefficient, K'' and flow behavior index, n''.

9.12 CONCLUSIONS

TTSP can be used for food and biopolymer to elucidate the structural change/deformation at selected temperature. The novelty of the principle is associated with the fact that the frequency and time domain of the viscoelastic properties can be extended to higher range. The TTSP produces master curves under given stresses and the corresponding temperature shift factor is dependent on the stress level at which the time shifting is used. TTSP plots for the biopolymers like PLA show some overlap at higher frequencies but significant dispersion at low frequencies due to longer thermal exposures. MCC plot or Han plot could also describe the TTS effect for food and biopolymers, effectively.

REFERENCES

Ahmed, J., 2012. Applicability of time–temperature superposition principle: dynamic rheology of mung bean starch blended with sodium chloride and sucrose—part 2. J. Food Eng. 109, 329–335.

Ahmed, J., 2015. Effect of barley β-glucan concentrate on oscillatory and creep behavior of composite wheat flour dough. J. Food Eng. 152, 85–94.

Ahmed, J., Auras, R., Kijchavengkul, T., Varshney, S.K., 2012. Rheological, thermal and structural behavior of poly(ε-caprolactone) and nanoclay blended films. J. Food Eng. 111, 580–589.

Ahmed, J., Varhney, S.K., Auras, R., Hwang, S.W., 2010. Thermal and rheological properties of L-polylactide/polyethylene glycol/silicate nanocomposites films. J. Food Sci. 75, N97–N108.

Ahmad, F.B., Williams, P.A., 1999. Effect of salts on the gelatinization and rheological properties of sago starch. J. Agric. Food Chem. 47 (8), 3359–3366.

Aleksandrov, A.P., Lazurkin, Y.S., 1939. Zh. Tekh. Fiz. 9, 1249.

Al-Ruqaie, I.M., Kasapis, S., Richardson, R.K., Mitchell, G., 1997. The glass transition zone in high solids pectin and gellan preparations. Polymer 38, 5685–5694.

Alwis, K.G.N.C., Burgoyne, C.J., 2006. Time-temperature superposition to determine the stress rupture of aramid fibres. Appl. Compos. Mater. 13, 249–264.

Alwis, K.G.N.C., Burgoyne, C.J., 2008. Accelerated creep testing for aramid fibres using the stepped isothermal method. J. Mater. Sci. 43, 4789–4800.

Arrhenius, S., 1889. Translated into English in selected readings in chemical kinetics. In: Back, M.H., Laidler, K.J. (Eds.), Oxford, NY, 1967. Z. Phys. Chem. 4, 226.

Baek, D.M., Han, C.D., 1995. Rheological behavior of binary mixtures of polystyrene-block-polyisoprene copolymers in the disordered state. Polymer 36, 4833–4839.

Chin, N.L., Chan, S.M., Yusof, Y.A., Chuah, T.G., Talib, R.A., 2009. Modelling of rheological behaviour of pummelo juice concentrates using master-curve. J. Food Eng. 93, 134–140.

Cole, K.S., Cole, R.S., 1941. Dispersion and adsorption in dielectrics: I. Alternating current characteristics. J. Chem. Phys. 9, 341–351.

da Silva, J.A.L., Gonçalves, M.P., Rao, M.A., 1994. Influence of temperature on the dynamic and steady-shear rheology of pectin dispersions. Carbohydr. Polym. 23 (77), 87.

Dealy, J.M., Wissbrun, K.F., 1999. Introduction to nonlinear viscoelasticity. In: Wissbrun, K., Dealy, J.M. (Eds.), Melt Rheology and Its Role in Plastics Processing: Theory and Applications. Kluwer Academic Publication Dordrecht, Dordrecht, pp. 103–152.

Edwards, S.F., 1967. The statistical mechanics of polymerized material. Proc. Phys. Soc. 92, 9.

Ferry, J.D., 1980. Viscoelastic properties of polymers. John Wiley & Sons, New York, NY, p. 640.
Han, C.D., Jhon, M.S., 1986. Correlations of the first normal stress difference with shear stress and of the storage modulus with loss modulus for homopolymers. J. Appl. Polym. Sci. 32, 3809–3840.
Han, C.D., 1988. The influence of molecular weight distribution on the linear viscoelastic properties of polymer blends. J. Appl. Polym. Sci. 35, 167.
Han, C.D., Kim, J.K., 1993. On the use of time-temperature superposition in multicomponent/multiphase polymer systems. Polymer 34, 2533–2539.
Han, C.D., Kim, Y.J., Chuang, H.K., Kwack, T.H., 1983. Rheological properties of branched low-density polyethylene. J. Appl. Polym. Sci. 28, 3435.
Han, C.D., Ma, Y.J., Chu, S.G., 1986. Rheological behavior of partially hydrolyzed poly(vinyl acetate-*co*-ethylene). J. Appl. Polym. Sci. 32, 5597.
Han, C.D., Kim, J., Kim, J.K., 1989. Determination of the order–disorder transition temperature of block copolymers. Macromolecules 22, 383–394.
Handge, U., Pötschke, P., 2007. Deformation and orientation during shear and elongation of a polycarbonate/carbon nanotubes composite in the melt. Rheol. Acta 46 (6), 889–898.
Kasapis, S., Al-Marhoobi, I.M.A., Khan, A.J., 2000. Viscous solutions, networks and the glass transition in high sugar galactomannan and κ-carrageenan mixtures. Int. J. Biol. Macromol. 27, 13–20.
Kracalik, M., Laske, S., Witschnigg, A., Holzer, C., 2011. Elongational and shear flow in polymer-clay nanocomposites measured by on-line extensional and off-line shear rheometry. Rheol. Acta 50, 937–944.
Lakes, R.S., 2004. Viscoelastic measurement techniques. Rev. Sci. Instrum. 75, 797–810.
Leaderman, H., 1943. Elastic and Creep Properties of Filamentous Materials and Other High Polymers. The Textile Foundation, Washington, DC.
Luo, W., Ting-Qing, Y., Qunli, A., 2001. Time-temperature-stress equivalence and its application to nonlinear viscoelastic materials. Acta Mech. Solida Sin. 14, 195–199.
Luo, W., Wang, C., Hu, X., Yang, T., 2012. Long-term creep assessment of viscoelastic polymer by time-temperature-stress superposition. Acta Mech. Solida Sin. 25 (6), 571–578.
Markovitz, H., 1975. Superposition in rheology. J. Polym. Sci. C 50, 431–456.
Mendieta-Taboada, O., Sobralb, P.J.A., Carvalho, R.A., Habitante, A.M.B.Q., 2008. Thermomechanical properties of biodegradable films based on blends of gelatin and poly(vinyl alcohol). Food Hydrocoll. 22 (8), 1485–1492.
Meng, L., Dong, L., Wang, L., Adhikari, B., 2015. Creep behavior of starch-based nanocomposite films with cellulose nanofibrils. Carbohydr. Polym. 117, 957–963.
Meza, B.E., Verdinia, R.A., Rubiolo, A.C., 2012. Temperature dependency of linear viscoelastic properties of a commercial low-fat soft cheese after frozen storage. J. Food Eng. 109, 475–481.
Muliawan, E.B., Hatzikiriakos, S.G., 2007. Rheology of mozzarella cheese. Int. Dairy J. 17, 1063–1072.
Nakada, M., Miyano, Y., Cai, H., Kasamori, M., 2011. Prediction of long-term viscoelastic behavior of amorphous resin based on the time-temperature superposition principle. Mech. Time-Depend. Mater. 15, 309–316.
Narimissa, E., Gupta, R.K., Kao, N., Choi, H.J., Jollands, M., Bhattacharya, S.N., 2014. Melt rheological investigation of polylactide-nanographite platelets biopolymer composites. Polym. Eng. Sci. 54 (1), 175–188.
Nickerson, M.T., Paulson, A.T., Speers, R.A., 2004. A time–temperature rheological approach for examining food polymer gelation. Trends Food Sci. Technol. 15, 569–574.

Nickerson, M.T., Paulson, A.T., Speers, R.A., 2007. Time–temperature studies of gellan polysaccharide–high sugar mixtures: effect of sodium ions on structure formation. J. Food Sci. 72 (5), E315–E319.

Nikolic, M.S., Mitric, M., Dapcevic, A., Djonlagic, J., 2016. Viscoelastic properties of poly(ε-caprolactone)/clay nanocomposites in solid and in melt state. J. Appl. Polym. Sci. 133, E315–E319.

Palade, L.I., Verney, V., Attane, P., 1995. Time–temperature superposition and linear viscoelasticity of polybutadienes. Macromolecules 28, 7051–7057.

Povolo, F., Fontelos, M., 1987. Time-temperature superposition principle and scaling behavior. J. Mater. Sci. 22, 1530–1534.

Ptaszek, A., Berski, W., Ptaszek, P., Witczak, T., Repelewicz, U., Grzesik, M., 2009. Viscoelastic properties of waxy maize starch and selected non-starch hydrocolloid gels. Carbohydr. Polym. 76, 567–577.

Ptaszek, P., Grzesik, M., 2007. Viscoelastic properties of maize starch and guar gum gels. J. Food Eng. 82 (2), 227–237.

Quek, M.C., Chin, N.L., Yusof, Y.A., 2013. Modeling of rheological behaviour of soursop juice concentrates using shear rate–temperature–concentration superposition. J. Food Eng. 118, 380–386.

Reichert, P., Hoffmann, B., Bock, T., Thomann, R., Mulhaupt, R., Friedrich, C., 2001. Morphological stability of poly(propylene) nanocomposites. Macromol. Rapid Commun. 22 (7), 519–523.

Singh, A.P., Lakes, R.S., Gunasekaran, S., 2006. Viscoelastic characterization of selected foods over an extended frequency range. Rheol. Acta 46, 131–142.

Solomon, M.J., Almusallam, A.S., Seefeldt, K.F., Somwangthanaroj, A., Varadan, P., 2001. Rheology of polypropylene/clay hybrid materials. Macromolecules 34, 1864–1872.

Subramaninan, R., Gunasekaran, S., 1997. Small amplitude oscillatory shear studies on mozarella cheese. Part II. Relaxation spectrum. J. Texture Stud. 28, 643.

Tschoegl, N.W., Knauss, W.G., Emri, I., 2002. The effect of temperature and pressure on the mechanical properties of thermo- and/or piezorheologically simple polymeric materials in thermodynamic equilibrium—a critical review. Mech. Time-Depend. Mater. 6, 53–99.

Udyarajan, C.T., Horne, D.S., Lucey, J.A., 2007. Use of time-temperature superposition to study the rheological properties of cheese during heating and cooling. Int. J. Food Sci. Technol. 42, 686–698.

Urzhumtsev, Y.S., 1972. Time-temperature superposition, review. Mekhan. Polim. 3, 498.

van Gurp, M., Palmen, J., 1998. Time temperature superposition for polymeric blends. Rheol. Bull. 67, 5–8.

Woirgard, J., Sarrazin, Y., Chaumet, H., 1977. Apparatus for the measurement of internal friction as a function of frequency between 1 and 10 Hz. Rev. Sci. Instrum. 48, 1322.

Wu, D., Wu, L., Zhang, M., 2007. Rheology of multi-walled carbon nanotube/poly(butylene terephthalate) composites. J. Polym. Sci. B 45 (16), 2239–2251.

Yang, T.-C., Wu, T.-L., Hung, K.-C., Chen, Y.-L., Wu, J.-H., 2015. Mechanical properties and extended creep behavior of bamboo fiber reinforced recycled poly(lactic acid) composites using the time–temperature superposition principle. Constr. Build. Mater. 93 (15), 558–563.